

## ( $d,p$ - $f$ ) Angular-Correlation Study of Fission-Barrier Transition States : Energy Gap of a Highly Deformed Nucleus\*

HAROLD C. BRITT, WILLIAM R. GIBBS, JAMES J. GRIFFIN, AND RICHARD H. STOKES  
*University of California, Los Alamos Scientific Laboratory, Los Alamos, New Mexico*

(Received 23 February 1965)

The ( $d,p$ ) reaction was used to produce fissioning nuclei with excitations from the fission threshold to 5 MeV above. The angular correlation of the fission fragments and the reaction protons has been measured as a function of excitation. A theoretical correlation function is developed to permit values of the parameter  $K_0^2$  to be derived from the observed angular anisotropy. For a Pu<sup>239</sup> target the values obtained for  $K_0^2$  show a stepwise increase with increasing excitation. The largest step occurs at  $\sim 2.6$  MeV above the fission threshold, and is interpreted as the beginning of quasiparticle excitations of the highly deformed fissioning nucleus. On this basis the pairing energy gap appears to be significantly increased for large nuclear deformations. Also,  $K_0^2$  is observed to change at  $\sim 0.7$  and  $\sim 1.6$  MeV above threshold. It is suggested that these energies are the onset of collective vibrational transition states through which fission occurs.

### 1. INTRODUCTION

THE ( $d,p$ ) reaction has been used in a previous experiment<sup>1</sup> to measure the probability of fission as a function of excitation energy. It was shown that fission thresholds can be measured for target nuclei which undergo thermal neutron-induced fission. For these nuclei, the ( $d,p$ ) reaction produces even-even fissioning nuclei with excitation energies near the fission threshold, a region of excitation energy which is inaccessible to neutron-induced fission experiments.

Another property of the ( $d,p$ ) reaction is that fissioning nuclei can be formed in states of moderately high angular momentum, so that it is possible to investigate the angular correlations of the fragments at excitation energies near the fission threshold. For high excitations, the results of anisotropy theory<sup>2</sup> for fission induced by particle capture show that the anisotropy is an increasing function of the average angular momentum of the fissioning nucleus and a decreasing function of the amount of excitation above the fission threshold. Because the ( $d,p$ ) reaction can transfer considerable angular momentum and at the same time induce fission with minimum excitation, large correlation effects may be anticipated. A measurement of these correlations as a function of excitation energy reveals information on the transition states of the nucleus as it passes over the fission barrier.<sup>2</sup> These transition states consist of collective and particle excitations of the fissioning nucleus at the saddle-point deformation. Of particular interest

are measurements for fissioning nuclei throughout a band of several MeV above threshold, because in this region superfluidity effects due to nuclear pairing<sup>3</sup> are most important. At these low excitation energies it is possible to observe effects which distinguish the finite isolated nuclear superfluid<sup>4</sup> from the infinite systems which are usually considered.<sup>5,6</sup> In particular, it was expected that the angular correlation should show a discontinuity at the excitation energy corresponding to the onset of two quasiparticle excitations. In the threshold region, evidence for the opening of new transition states has been seen in the previous measurements<sup>1</sup> of fission-barrier penetrability. In the penetrability data, because of competition from neutron emission and the effect of deuteron breakup, only a range of about 1.6 MeV was accessible to clear interpretation. The present anisotropy measurements are insensitive to the above two obscuring effects and permit unambiguous interpretation over a wider excitation range.

In the present experiment, measurements were made of the angular correlations of fragments emitted in the fission of Pu<sup>240</sup> and U<sup>234</sup>. The results for Pu<sup>240</sup> clearly show the expected nuclear pairing effects, and also show evidence for low-lying collective excitations near the fission threshold.

### 2. EXPERIMENTAL PROCEDURES

The experimental method was similar to that used in the previous determination of fission thresholds.<sup>1</sup> Semiconductor fission detectors were situated in a plane defined by the incoming 14.9-MeV deuteron beam and the observed reaction protons. The proton detector con-

\* Work done under the auspices of the U. S. Atomic Energy Commission.

<sup>1</sup> J. A. Northrop, R. H. Stokes, and K. Boyer, *Phys. Rev.* **115**, 1277 (1959).

<sup>2</sup> A. Bohr, *Proceedings of the International Conference on the Peaceful Uses of Atomic Energy, Geneva, 1955* (United Nations, New York, 1956), Vol. 2; I. Halpern and V. M. Strutinskii, *Proceedings of the Second United Nations International Conference on the Peaceful Uses of Atomic Energy, Geneva, 1958* (United Nations, Geneva, 1958), Vol. 15; J. Griffin, *Proceedings of the International Conference on Nuclear Physics, Paris, 1958* (Dunod Cie., Paris, 1958); *Phys. Rev.* **116**, 107 (1959); **127**, 1248 (1962); *Proceedings of the International Conference on Nuclear Structure, 1960*, edited by D. A. Bromley and E. W. Vogt (University of Toronto Press, Toronto, 1960). V. M. Strutinskii, *Nucl. Phys.* **27**, 348 (1961).

<sup>3</sup> A. Bohr, B. R. Mottelson, and D. Pines, *Phys. Rev.* **110**, 936 (1958); S. T. Belyaev, *Kgl. Danske Videnskab. Selskab, Mat. Fys. Medd.* **31**, No. 11 (1959); in *The Many Body Problem*, edited by C. DeWitt (John Wiley & Sons, Inc., New York, 1959), p. 377; B. R. Mottelson, in *The Many Body Problem*, edited by C. DeWitt (John Wiley & Sons, Inc., New York, 1959), p. 283; J. Griffin and M. Rich, *Phys. Rev.* **118**, 850 (1960); S. G. Nilsson and O. Prior, *Kgl. Danske Videnskab. Selskab, Mat. Fys. Medd.* **32**, No. 16 (1960); and other references too numerous to list.

<sup>4</sup> M. Rich and J. Griffin, *Phys. Rev. Letters* **11**, 19 (1963).

<sup>5</sup> D. W. Lang, *Nucl. Phys.* **42**, 353 (1963).

<sup>6</sup> J. Griffin, *Phys. Rev.* **132**, 2204 (1963); **135**, AB2(E) (1964).

sisted of a semiconductor transmission  $\Delta E$  detector followed by a semiconductor  $E$  detector in which the protons stopped. The pulses from the two detectors were used with an analog computer<sup>7</sup> to distinguish protons from other emitted particles.

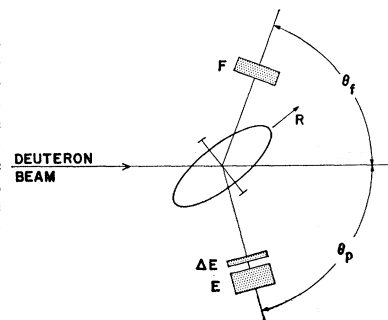
A fast-slow coincidence system was used to identify protons in coincidence with fission. A fast coincidence with  $\tau = 50$  nsec was required between the fission detector and the  $E$  detector, and a slow coincidence was required with the proton identification system. A pulse from the coincidence system was used to gate a multi-channel analyzer which recorded a pulse height proportional to the sum of the pulses in the  $\Delta E$  and  $E$  detectors (i.e., proportional to the proton energy). In one set of measurements, three fission detectors were used simultaneously to determine the coincident counting rate for three different fission angles. In this case, three coincidence systems were used to gate three separate 100-channel blocks of a 400-channel analyzer.

During the measurements a simultaneous determination of the chance coincidence contribution to the spectra was made. This was done using another coincidence system which was identical to that used for the true spectra except that the signal from the  $E$  detector was delayed by about 160 nsec (2 cyclotron periods) from true coincidence. The chance spectra were also recorded in a 100-channel block of the analyzer. In the measurement where three fission detectors were used, only one of the chance spectra was recorded and for the other two detectors the total number of chance counts was recorded on scalars. In the analysis of the data, it was assumed that the shape of the chance spectrum was the same for each fission angle. During the measurements, the chance rates were typically 5% of the true rates.

The deuteron beam, which was obtained from the Los Alamos variable-energy cyclotron, had a mean energy of 14.9 MeV. The beam energy was determined by slowing the deuterons with aluminum absorbers and comparing the solid-state-detector response of the degraded beam to the response of 5.1-MeV alpha particles. The proton energy scale was calibrated using the elastically scattered deuteron group from Pu and U, and proton groups from the  $(d,p)$  reaction on C<sup>12</sup> and O<sup>16</sup>. The over-all width of the response in the energy-measuring channel was 200 keV full-width at half-maximum. This width includes deuteron-beam energy spread, detector response, noise, and kinematic broadening. The targets were prepared by vacuum evaporation of Pu<sup>239</sup>O<sub>2</sub> and U<sup>238</sup>O<sub>2</sub> onto 60- $\mu\text{g}/\text{cm}^2$  carbon backings. The Pu<sup>239</sup> and U<sup>238</sup> deposits had thicknesses of 175 and 360  $\mu\text{g}/\text{cm}^2$ , respectively.

The data were analyzed by first correcting each spectrum for the chance contribution. The results were transformed to the center-of-mass system of the fissioning nucleus. This transformation was performed using values for the recoil velocity and angle of the fissioning

FIG. 1. Schematic drawing of the experimental arrangement.  $R$  designates the direction of the recoiling excited nucleus from which the fission fragments arise, and the ellipse suggests the fragment angular distribution for a fixed proton momentum.



compound nucleus that were calculated from the deuteron energy, and the energy and angle of the proton. The transformation was performed assuming that all the fragments have a single mass and a single energy. The fragment mass was taken as one-half the mass of the fissioning nucleus and the fragment energy was taken as the mean kinetic energy measured for thermal neutron-induced reactions forming the same fissioning nuclei.<sup>8</sup>

### 3. EXPERIMENTAL RESULTS

There were two types of measurements performed to obtain the results presented here. In the first measurement, a single fission detector was used with the Pu<sup>239</sup> target, and measurements were made for various angles of the fission detector in order to determine the detailed shape of the angular correlation. This type of measurement is illustrated schematically in Fig. 1. In the second set of measurements, three detectors were placed at fixed laboratory angles of +20, +110, and +155 deg with respect to the beam. With this arrangement, a series of runs were taken to obtain the best possible statistical accuracies on the anisotropy measurements as a function of the proton energy.

The coincident proton-energy spectra which were obtained in the measurements with the three fixed detectors are shown in Fig. 2. These spectra are the sum of the coincident spectra measured for the three fission detectors. The spectra shown in Fig. 2 have essentially the same shape as those obtained in the previous measurement.<sup>1</sup> The arrows shown in Fig. 2 represent the definition of the proton energy corresponding to the excitation energy at the fission threshold. These positions for the threshold energy were obtained<sup>9</sup> by comparing the shapes of the coincident proton energy spectra with the spectra obtained in the previous threshold measurements.<sup>1</sup> As in the previous measurements<sup>1</sup> the threshold is defined as the energy at which the fission probability

<sup>8</sup> J. C. D. Milton and J. S. Fraser, Can. J. Phys. **40**, 1626 (1962).

<sup>9</sup> The equivalent neutron energies at threshold as defined from the data of Fig. 2 are more negative by about 200 keV than the results of the previous measurement (Ref. 1). This discrepancy is within the uncertainties of the proton-energy calibrations and does not affect the  $E^* - E_f$  energy scale.

<sup>7</sup> R. H. Stokes, Rev. Sci. Instr. **31**, 768 (1960).

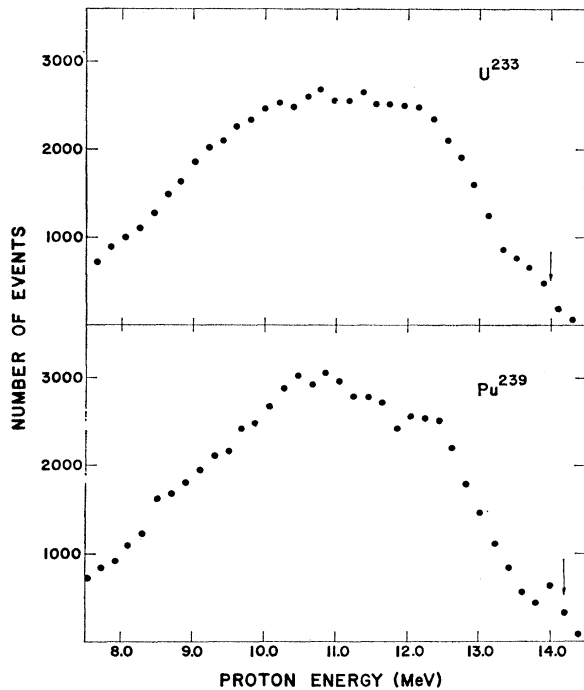


FIG. 2. Spectra of protons ( $\theta_p = -140^\circ$ ) coincident with fission fragments. These data are the sum of the spectra obtained with  $\theta_f = +20^\circ, +110^\circ, \text{ and } +155^\circ$ .

reached 50% of its first plateau value.<sup>10</sup> These thresholds were then used to obtain the  $E^* - E_{th}$  scale of excitation energy above the fission threshold used in the following figures.

Figure 3 shows the angular correlations obtained in the first measurement with the single fission detector for the  $\text{Pu}^{239}$  target. In this figure, results are shown for intervals of the excitation energy above the fission threshold of 0–1, 1–2, and 2–3 MeV for laboratory proton angles of  $140^\circ$  and  $75^\circ$ . The center-of-mass angles are measured relative to the classical recoil angle of the fissioning nucleus produced in the  $(d, p)$  reaction. The values of these recoil angles for the threshold excitation are indicated on the figure. Both positive and negative angles<sup>11</sup> are shown in Fig. 3 in order to demonstrate that within the statistical accuracies the classical recoil angle is the symmetry angle for the angular correlations. The solid lines shown in Fig. 3 represent least-squares fits of the experimental results to the function

$$W(\theta) \propto 1 + g_2 P_2(\cos \theta). \quad (1)$$

<sup>10</sup> L. N. Usachev, V. A. Pavlinchuk, and N. S. Rabotnov, Zh. Eksperim. i Teor. Fiz. 17, 1312 (1963) [English transl.: Soviet Phys.—JETP 44, 1950 (1963)] point out an alternative prescription for the threshold. Their estimate of the difference between the two interpretations is, however, exaggerated by the large value of  $E_{curv}$  ( $=0.800$  MeV) they assume. A value  $E_{curv} \leq 0.350$  MeV, as is indicated by the results of Ref. 1, reduces the change in threshold to less than 0.2 MeV. Cf. also Ref. 18.

<sup>11</sup> In the layout shown in Fig. 1, positive angles are measured in a clockwise direction from the recoil angle and negative angles in a counter-clockwise direction.

It is seen that within the experimental uncertainties this function gives an adequate fit to the results. The results shown in Fig. 3 illustrate three general characteristics of the angular correlations: (1) the anisotropies  $W(0^\circ)/W(90^\circ)$  decrease by approximately a factor of 2 for every 1 MeV of excitation energy above the threshold, (2) the maximum anisotropy is 2.8 for the  $140^\circ$  proton angle and 2.0 for the  $75^\circ$  proton angle, and (3) as discussed above, the symmetry angle for the angular correlation is close to the classical recoil angle of the fissioning nucleus.

Following the above experiment, measurements were made with much higher statistical accuracy using three fixed fission detectors and collecting data at the three angles simultaneously. In this measurement the proton detector was placed at  $140^\circ$  because of the larger anisotropies and because the theoretical interpretation was more straightforward for a backward proton angle (see Sec. 4). With this arrangement data were taken for both  $\text{Pu}^{239}$  and  $\text{U}^{233}$  targets.

The results were fitted to Eq. (1) and the values obtained for  $g_2$  are shown in Fig. 4. In the energy interval 0–5 MeV above the threshold excitation, approximately  $1 \times 10^5$  and  $5 \times 10^4$  events were recorded for the  $\text{Pu}^{239}$  and  $\text{U}^{233}$  targets, respectively. The  $\text{Pu}^{239}$  data are therefore statistically superior to those for  $\text{U}^{233}$ . Figure 3 shows that near threshold the anisotropies for the  $\text{U}^{233}$  target are approximately a factor of 2 less than for the  $\text{Pu}^{239}$  target. For this reason also, the  $\text{Pu}^{239}$  data provide more precise information on the nuclear structure at the fission barrier. These data therefore provide the basis for most of the conclusions in this paper.

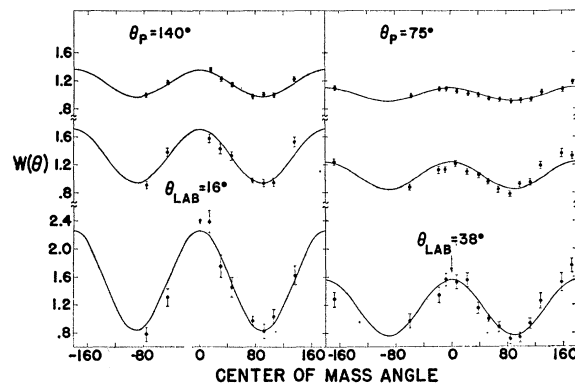


FIG. 3. Angular correlations taken with a single fission detector for a  $\text{Pu}^{239}$  target. For laboratory proton-scattering angles of  $75^\circ$  and  $140^\circ$ , the angular distribution of fission fragments is shown for various intervals of the excitation energy above the fission threshold. The lower two curves are for 0–1-MeV excitation, the middle two curves for 1–2-MeV excitation, and the upper two curves for 2–3-MeV excitation. The angular scale is taken relative to the recoil direction of the excited fissioning nucleus.  $\theta_{lab}$  designates the value of the laboratory recoil angle for the two values of  $\theta_p$ .

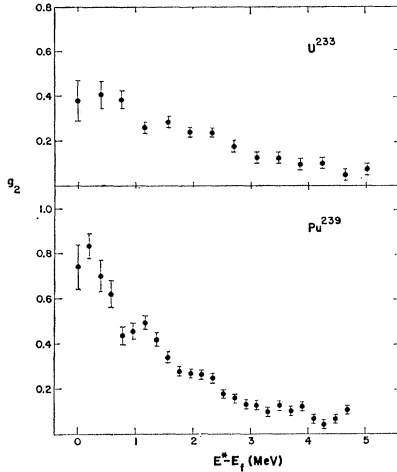


FIG. 4. Measured values of the coefficient  $g_2$  for  $U^{238}$  and  $Pu^{239}$  targets. These values were derived from data taken with three fixed fission detectors and with  $\theta_p = 140^\circ$ .

#### 4. THEORY

We now turn to the theoretical treatment of the  $(d, p-f)$  angular correlations. Our analysis is based on the simplest possible assumptions, apart from the fact that relative cross sections for various angular momenta are computed from distorted-wave Born-approximation (DWBA) theory. The assumptions are as follows:

(1) Stripping occurs only into states which can be formed from the unexcited ground state of the target plus a single neutron in one of the (spherical)  $N=7$  shell-model states.

(2) All such states are assumed to be available at every excitation energy, and their average reduced widths to compound states are assumed constant in energy.

(3) The average probability that a compound state fissions through a transition state with a given value of  $K$  is assumed proportional to  $\exp(-K^2/2K_0^2)$ , where  $K_0^2$  is the energy-dependent quantity finally to be extracted from the data.

The resulting analysis is detailed in the paragraphs which follow.

To compute the angular distribution of fission fragments from the  $(d, p-f)$  reaction, we need the amplitudes (a) for formation of a compound nucleus in a state  $(J, J_z, \lambda)$  when the proton is observed with momentum  $\mathbf{k}_p$  and (b) for fission of the compound nucleus from the compound state with fragments emitted into the solid angle  $\hat{\theta}_f$ . Then

$$W(\hat{\theta}_f, \mathbf{k}_p) = \left| \sum_{J, J_z, \lambda} A(\mathbf{k}_p; J, J_z, \lambda) B(\hat{\theta}_f; J, J_z, \lambda) \right|^2 \quad (2)$$

is the angular correlation of the fragments with the proton. A sum over final spin projections and an average

over initial spin projections is implicit in all relevant expressions.

To compute the stripping amplitude, we assume that the neutron is captured into a compound state  $(J, J_z, \lambda)$  via a single-particle state  $(l, j, m)$  coupled to the unexcited core whose angular momentum  $(I, I_z)$  is equal to the angular momentum of the target nucleus. Then

$$A(\mathbf{k}_p; J, J_z, \lambda) = \sum_{l, j, m} A(l, j, m; I, I_z; J, J_z; \mathbf{k}_p) \gamma_{lj}^{J\lambda}, \quad (3)$$

where  $\gamma_{lj}^{J\lambda}$  is the reduced width for the compound state  $(J, \lambda)$  and  $A(l, j, m; I, I_z; J, J_z; \mathbf{k}_p)$  is to be computed from an appropriate stripping calculation.

To compute the fragment angular distribution from the compound state  $(J, J_z, \lambda)$  we assume that a fission through a transition state  $(J, J_z, K)$  emits fragments into the angle  $\hat{\theta}_f$  with an amplitude given by the normalized symmetric top wave function  $\mathcal{D}_{J_z K}^{J'}(\hat{\theta}_f)$  which describes the orientation of the fissioning nucleus as it passes over the fission barrier,<sup>2</sup> and that the amplitude for the compound state  $(J, \lambda)$  to decay through a transition state with projection  $K$  of angular momentum along the nuclear symmetry axis is  $b_K^{J\lambda}$ . Then

$$B(\hat{\theta}_f; J, J_z, \lambda) = \sum_K b_K^{J\lambda} \mathcal{D}_{J_z K}^{J'}(\hat{\theta}_f). \quad (4)$$

In the present experiment the sum over  $\lambda$  in Eq. (2) involves many states of a given  $J$  value because of the experimental resolution ( $\sim 200$  keV) and the narrow spacing of the relevant compound levels ( $\sim 100$  eV). One is therefore justified in the approximation

$$\begin{aligned} \sum_{\lambda\lambda'} b_K^{J\lambda} b_{K'}^{J\lambda'} \gamma_{lj}^{J\lambda} \gamma_{l'j'}^{J\lambda'} \\ = \sum_{\lambda} |b_K^{J\lambda}|^2 |\gamma_{lj}^{J\lambda}|^2 \delta_{KK'} \delta_{ll'} \delta_{jj'} \delta_{JJ'} \\ = \langle |b_K^{J\lambda}|^2 \rangle_{\text{av}} \langle \gamma^2 \rangle_{\text{av}} \delta_{KK'} \delta_{ll'} \delta_{jj'} \delta_{JJ'} N(J, l, j), \end{aligned} \quad (5)$$

where  $N(J, l, j)$  is the number of single-particle states with quantum numbers  $(J, l, j)$  and  $\langle \gamma^2 \rangle_{\text{av}}$  is the average reduced width for such single-particle states.

We shall assume that from each single-particle state  $(l, j)$  every  $J$  state allowed by angular-momentum coupling to the target spin is available. Then  $N(J, l, j) = N_1(J, j) N_2(l, j)$ , where  $N_1(J, j) = \Delta(j, I, J)$  and  $N_2(l, j)$  is still to be specified on physical grounds.  $\Delta(abc)$  is one if  $a, b, c$  satisfy the triangular inequalities; zero, otherwise. The angular distribution is then a simple sum over products of density matrices:

$$\begin{aligned} W(\mathbf{k}_p, \hat{\theta}_f) \propto \sum_{J, l, j, K} \langle |b_K^{J\lambda}|^2 \rangle_{\text{av}} N_1(J, j) N_2(l, j) \\ \times \left\{ \sum_{J_z J_z'} E_{(d,p)}^{J_z J_z'}(\mathbf{k}_p; J, l, j) E_{\text{fission}}^{J_z J_z'}(\hat{\theta}_f; J, K) \right\}, \end{aligned} \quad (6)$$

where

$$E_{\text{fission}}^{J_z J_z'}(\hat{\theta}_f; J, K) = \mathcal{D}_{J_z, K}^{J*}(\hat{\theta}_f) \mathcal{D}_{J_z', K}^J(\hat{\theta}_f) \quad (7)$$

and

$$E_{(d,p)}^{J_z J_z'}(\mathbf{k}_p; J) = \sum_{mm'} A^*(ljm; I, I_z; J, J_z; \mathbf{k}_p) \times A(ljm'; I, I_z; J, J_z'; \mathbf{k}_p) \quad (8)$$

is the usual density matrix for stripping a neutron ( $l, j$ ) into a single-particle state  $J$ .

Equation (6) states that the full angular correlation function is a sum over angular correlations for various possible  $j, l, J, K$  values weighted with the relative probability  $\langle |b_{K^J}|^2 \rangle_{\text{av}} N(J, l, j)$  that the compound nucleus is formed through a state ( $j, l, J$ ) and decays through a transition state  $K$ .

To reduce Eq. (6) to an easily calculable form we first expand  $E_{\text{fission}}^{J_z J_z'}$  in statistical tensors:

$$E_{\text{fission}}^{J_z J_z'} = \sum_{LM} Y_L^M(\theta_f, \varphi_f) [4\pi(2L+1)]^{1/2} \times (LJOK | LJJK) (LJM J_z' | LJJ J_z) (1/8\pi^2). \quad (9)$$

The sum over  $K$  is now quite simple, and if one assumes  $\langle |b_{K^J}|^2 \rangle_{\text{av}} = \langle |b_{-K^J}|^2 \rangle_{\text{av}}$ , it has the property:

$$\sum_K \langle |b_{K^J}|^2 \rangle_{\text{av}} (LJOK | LJJK) = 0, \quad L \text{ odd} \quad (10)$$

so that only even  $L$  need be considered.

The analogous expansion of  $E_{(d,p)}^{J_z J_z'}(l, j, J; \mathbf{k}_p)$  is given by Satchler<sup>12</sup> for plane waves and by Huby, Refai, and Satchler<sup>13</sup> for distorted waves. The notation used in the present paper differs from that given by these authors.

$$E_{(d,p)}^{J_z J_z'}(l, j, J; \mathbf{k}_p) = \sum_{L'M'} (L'JM' J_z | L'JJ J_z') \eta_{L'}(IljJ) \rho_{L'l}^{M'}(\mathbf{k}_p), \quad (11)$$

where

$$\eta_L(IljJ) = W(Ll j \frac{1}{2}; lj) W(Lj J I; jJ) \times [(2J+1)(2l+1)]^{1/2} (2j+1)(2L+1) \quad (12)$$

and

$$\rho_{Ll}^M(\mathbf{k}_p) = \sum_{m, m'} (LLMm | Lllm') \beta_l^m(\mathbf{k}_p) \beta_l^{m'}(\mathbf{k}_p)^* \quad (13)$$

when no spin-orbit interaction is included. The double sum over  $J_z, J_z'$  can be rearranged into the Clebsch-Gordan orthogonality relationship, proportional to  $\delta_{L'L} \delta_{M'M'}$ . Thus  $L'$  is equal to  $L$  and, therefore, assumes only even values. We note also that

$$\rho_{0l}^0 = \sum_m |\beta_l^m(\mathbf{k}_p)|^2 = \sigma_l(\mathbf{k}_p), \quad (14)$$

where  $(2j+1)\sigma_l$  is proportional to the stripping cross section to a single-particle state characterized by  $l$  and

$j$ , and that for even  $L$ ,

$$(Ll00 | Lll0) W(Ll j \frac{1}{2}; lj) = \Delta(l \frac{1}{2} j) \Delta(Lll) \times (Lj0 \frac{1}{2} | Lj j \frac{1}{2}) [(2l+1)(2j+1)]^{-1/2}. \quad (15)$$

Then by defining  $\bar{\rho}$  by means of

$$\rho_{Ll}^M(\mathbf{k}_p) = (Ll00 | Lll0) \sigma_l(\mathbf{k}_p) \bar{\rho}_{Ll}^M(\mathbf{k}_p), \quad (16)$$

we obtain

$$W(\mathbf{k}_p, \hat{\theta}_f) \propto \sum_{LM} \sum_{l j J K} (2L+1)^{-1/2} g_L(jJIK) \times \Delta(l \frac{1}{2} j) \sigma_l(\mathbf{k}_p) (2J+1) \bar{\rho}_{Ll}^M(\mathbf{k}_p) \langle |b_{K^J}|^2 \rangle_{\text{av}} \times N_1(J, j) N_2(l, j) Y_L^{M*}(\hat{\theta}_f), \quad (17)$$

where

$$g_L(jJIK) = (2L+1) (LJ0K | LJJK) \times (Lj0 \frac{1}{2} | Lj j \frac{1}{2}) W(Lj J I; jJ) \times [(2j+1)(2J+1)]^{1/2}. \quad (18)$$

Equation (17) can now be reduced by the following summations over  $l, J$ , and  $K$ :

$$[(2j+1) \sum_l \sigma_l(\mathbf{k}_p) N_2(l, j) \bar{\rho}_{Ll}^M(\mathbf{k}_p)] \times [\sum_{l j'} (2j'+1) N_2(l, j') \sigma_l(\mathbf{k}_p)]^{-1} = d_{Lj}^M(\mathbf{k}_p), \quad (19)$$

$$[(2j+1)(2I+1)]^{-1} \sum_J (2J+1) N_1(J, j) \times \sum_K g_L(jJIK) \langle |B_{K^J}|^2 \rangle_{\text{av}} = g_L(j; I, \alpha), \quad (20)$$

where  $\alpha$  denotes one or more parameters describing the physical assumptions to be made concerning  $\langle |b_{K^J}|^2 \rangle_{\text{av}}$  and  $N_2(l, j)$ , and where

$$\langle |B_{K^J}|^2 \rangle_{\text{av}} = \langle |b_{K^J}|^2 \rangle_{\text{av}} [\sum_K \langle |b_{K^J}|^2 \rangle_{\text{av}}]^{-1}. \quad (20a)$$

Then the final result is

$$W(\mathbf{k}_p, \hat{\theta}_f) = (4\pi)^{1/2} \sum_{L, M, j} (2L+1)^{-1/2} \times g_L(j; I, \alpha) d_{Lj}^M(\mathbf{k}_p) Y_L^{M*}(\hat{\theta}_f). \quad (21)$$

To obtain numerical results, one has now to specify the physical assumptions to be made and carry through the computation of  $g_L(j; I, \alpha)$  and  $d_{Lj}^M(\mathbf{k}_p)$ . We have made the simplest possible assumptions concerning the available single-particle neutron states; namely, that all levels in the major oscillator shell,  $N=7$ , are available with equal probability at every excitation energy. This assumption is reasonable (a) because of the fact that the stable quadrupole deformation of the target results in significant mixing of the spherical levels so that various spherical eigenfunctions are already admixed into each deformed single-particle state, and (b) more than one single-particle state is being excited at any given experimental excitation energy, and finally (c) because at the excitation energies involved ( $\sim 5$  MeV) a given single-particle state is mixed significantly

<sup>12</sup> G. R. Satchler, Proc. Phys. Soc. (London) A66, 1081 (1953).  
<sup>13</sup> R. Huby, M. Y. Refai, and G. R. Satchler, Nucl. Phys. 9, 94 (1958).

into compound states<sup>14</sup> within an energy  $W \approx 2$  MeV, where  $W$  is the imaginary part of the neutron optical potential.<sup>15</sup> On all three counts a given spherical single-particle state will be excited over a wide range of experimental excitation energies, tending thereby to make applicable at every excitation energy the average properties of the whole collection of such states. In practice, this assumption implies that every odd  $l$  state ( $1 \leq l \leq 7$ ) is available with equal probability, so that  $N_2(l, j) = \Delta(l, j) \times \text{constant}$ . Since  $l$  is assumed to be odd only, there is associated with each value of  $j$  a unique value of  $l$ . Then  $\bar{\sigma}_j = \sum_l N_2(l, j) \sigma_l$  simplifies to  $\bar{\sigma}_j = \sigma_l(j)$ . The results would not be significantly modified if some (or all) even  $l$  values were included. The results are therefore not as restrictive as the odd- $l$  assumption might suggest.

The transition-state probability  $\langle |b_{K^J}|^2 \rangle_{\text{av}}$  is assumed to be proportional to the number of transition states available at the fission barrier at the specified excitation energy. For a Fermi-gas description of the transition state level density, one would have

$$\langle |b_{K^J}|^2 \rangle_{\text{av}} \propto \exp \left[ -\frac{\hbar^2}{2T} \left( \frac{1}{g_{J1}} [J(J+1) - K^2] + \frac{1}{g_{11}} K^2 \right) \right]. \quad (22)$$

For the nucleus highly deformed to the fission barrier, one expects  $g_{11} \gg g_{J1}$ , so that the form

$$\langle |b_{K^J}|^2 \rangle_{\text{av}} \propto \exp(-K^2/2K_0^2) \quad (23)$$

is an adequate first approximation.<sup>16</sup> Here  $K_0^2$  is an energy-dependent parameter which will be fit to experiment.

If the nuclear level density deviates from a simple Fermi-gas picture,<sup>6</sup> then  $K_0^2$  is expected to show deviations from the Fermi-gas prediction. It is in fact the dependence of  $K_0^2$  on excitation energy which is the primary object of the present experiment.

With these assumptions the coefficient  $g_L(j; I; K_0^2)$  can be computed, and there remains the computation of  $d_{Lj}^M(\mathbf{k}_p)$ .

To compute  $d_{Lj}^M(\mathbf{k}_p)$  we first consider the plane-wave approximation for the stripping process. Then apart from the constant factors the Butler amplitude (using surface evaluation) is

$$\beta_l^m = j_l(\kappa R) Y_l^m(\theta_\kappa, \varphi_\kappa) (2l+1)^{-1/2}, \quad (24)$$

where  $\theta_\kappa$  and  $\varphi_\kappa$  are the angles of the recoil momentum

vector  $\boldsymbol{\kappa} = \mathbf{k}_D - (M_I/M_F)\mathbf{k}_p$ . Then

$$\rho_{Ll}^M = j_l^2(\kappa R) (Ll00 | Ll00) (2L+1)^{-1/2} Y_L^M(\theta_\kappa, \varphi_\kappa) \quad (25)$$

and

$$d_{Lj}^M = (4\pi/(2L+1))^{1/2} Y_L^M(\theta_\kappa, \varphi_\kappa) \times ((2j+1)\bar{\sigma}_j/\sum_{j'}(2j'+1)\bar{\sigma}_{j'}). \quad (26)$$

Then

$$W(\theta_p, \varphi_p; \theta_f, \varphi_f) = \sum_L g_L(I; K_0^2) P_L(\cos \bar{\theta}_f), \quad (27)$$

where  $\bar{\theta}_f$  is measured from the recoil direction. The quantity  $g_L(I, K_0^2)$  is defined as

$$g_L(I, K_0^2) = \sum_j g_L(j; I, K_0^2) \bar{\sigma}_j / \sum_{j'} (2j'+1) \bar{\sigma}_{j'}. \quad (28)$$

One thus obtains a very simple angular correlation, exhibiting symmetry about the nuclear recoil direction.

In general, the plane-wave approximation is a poor one for stripping to heavy nuclei. The exception is the angular correlations it predicts for proton angles,  $140^\circ \lesssim \theta_p \lesssim 180^\circ$ . For angular properties of such back-angle processes, the plane-wave theory agrees quite well with the more complicated distorted-wave theory, although the cross sections  $\sigma_l$  do not agree at all. Thus for comparison with the present data ( $\theta_p = 140^\circ$ ) plane-wave theory suffices for calculating  $\bar{\rho}_{Ll}^M$ , whereas more accurate DWBA values must be used for  $\bar{\sigma}_j(\mathbf{k}_p)$ .

To demonstrate this we take  $g_4(I, K_0^2) \ll g_2(I, K_0^2)$  for a given value of  $J$ ,  $j$ , and  $l$ . This relative magnitude of  $g_4$  and  $g_2$  prevails in the present experimental data and is corroborated by calculation, which predicts  $g_4 \approx 0.1g_2$ . Then Eq. (21) becomes

$$W(\theta_p, \varphi_p; \theta_f, \varphi_f) = 1 + g_2(j; I, K_0^2) \times \sum_{M=-2}^{+2} d_{2j}^M(\mathbf{k}_p) Y_2^{M*}(\bar{\theta}_f). \quad (29)$$

For fixed values of  $\theta_p$ ,  $\varphi_p$ , each term in the sum expression can always be transformed by a simple rotation to the form

$$W(\theta_p, \varphi_p; \theta_f, \varphi_f = 0) = 1 + Q \cos 2(\theta_f - \theta_0), \quad (30)$$

where

$$Q(\mathbf{k}_p) = (3g_2(\gamma^2 + \beta^2)^{1/2} / (2 + g_2\alpha));$$

$$\tan 2\theta_0 = -\gamma/\beta$$

and

$$\alpha = \frac{1}{2}d_{2j}^0 + (\sqrt{\frac{3}{2}})d_{2j}^2,$$

$$\beta = \frac{1}{2}d_{2j}^0 - \frac{1}{\sqrt{6}}d_{2j}^2, \quad (31)$$

$$\gamma = (\sqrt{\frac{2}{3}})d_{2j}^1.$$

Then by direct calculation and comparison with the plane-wave theory, one finds that for each of the relevant  $j$  values ( $1/2 \leq j \leq 15/2$ ),  $Q$  and  $\theta_0$  approach the plane-wave value for  $\theta_p \geq \theta_c = 140^\circ$ . Examples for  $j = \frac{3}{2}$  and  $l = 1, 2$  are shown in Fig. 5. These cases were computed for  $K_0^2 = 0$  which guarantees  $g_L(j; I; K_0^2 = 0)$  equal to

<sup>14</sup> A. M. Lane, *Proceedings of the International Conference on the Nuclear Optical Model, Florida State University, Studies No. 32* (The Florida State University, Tallahassee, Florida, 1959).

<sup>15</sup> A. E. S. Green, *Proceedings of the International Conference on the Nuclear Optical Model, Florida State University, Studies No. 32* (The Florida State University, Tallahassee, Florida, 1959).

<sup>16</sup> J. Griffin, *Phys. Rev.* **127**, 1248 (1962); W. R. Gibbs and J. Griffin, *ibid.* **137**, B807 (1965); J. E. Simmons, R. B. Perkins, and R. L. Henkel, *ibid.* **137**, B809 (1965).

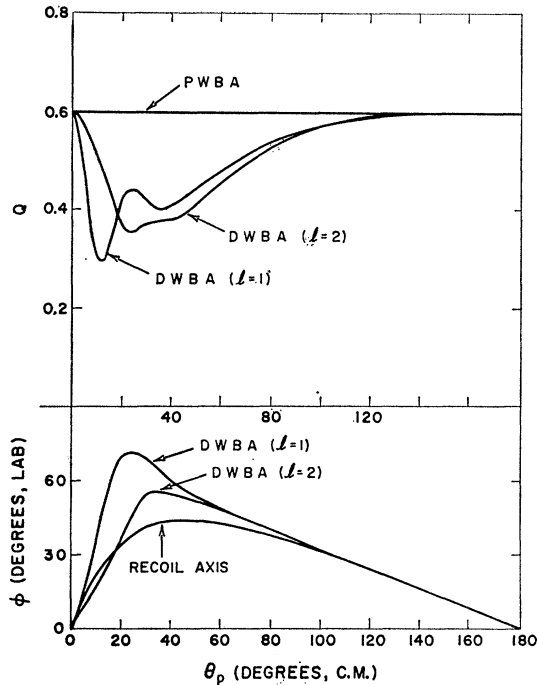


FIG. 5. A comparison of distorted- (DWBA) and plane-wave (PWBA) calculations for  $j = \frac{3}{2}$  and  $K_0^2 = 0$ . These curves illustrate the characteristic feature that for  $\theta_p \gtrsim 140^\circ$  the DWBA and PWBA give identical results for  $Q$  and  $\phi$ .

$g_L(jJI0)$  which is independent of  $J$ . The agreement in Fig. 5 therefore justifies the use of plane-wave theory in computing  $\bar{\rho}_{LI}^M$  for the present case. For  $\bar{\sigma}_j$ , however, the DWBA values have been used throughout.

Using Eqs. 28, 20, and 23 we have computed  $g_2(I, K_0^2)$  for  $I = \frac{1}{2}$  and  $I = \frac{5}{2}$  corresponding to  $\text{Pu}^{239}$  and  $\text{U}^{233}$ . These functions are plotted in Fig. 6.<sup>17</sup> From the

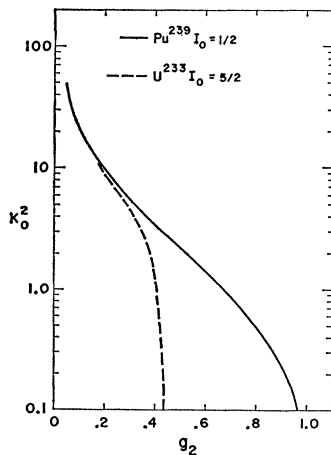


FIG. 6.  $K_0^2$  versus  $g_2$  calculated by means explained in the text. The difference between the curves results primarily from the difference in the target spins. This effect accounts adequately for the differences observed between the  $\text{U}^{233}$  and  $\text{Pu}^{239}$  data.

<sup>17</sup> Note added in proof. A semiclassical calculation of the relation between  $K_0^2$  and the fragment anisotropy from fission induced by a direct reaction has been received from V. M. Strutinskii, Kurchatov Institute of Atomic Energy Report No. IAE-733, 1964 (unpublished).

measured values of  $g_2$  one may then infer values of  $K_0^2$  as a function of excitation energy. These are shown in Fig. 7. It may be noted that  $K_0^2$  is near zero at the fission threshold as expected *a priori* for an even-even nucleus and that the values of  $K_0^2$  at higher excitation energies are in reasonable agreement with those measured independently by means of neutron induced fission.<sup>18,19</sup>

## 5. INTERPRETATION OF RESULTS

In a previous analysis of the energy dependence of the neutron- and alpha-particle-induced fission anisotropies, an estimate was obtained for the pairing-gap parameter  $\Delta_0$  in  $\text{Pu}^{240}$  distorted to its saddle-point shape:  $\Delta_0 = 1.16$  MeV.<sup>6</sup> This value is rather larger than that appropriate to  $\text{Pu}^{240}$  at its stable shape.<sup>20</sup> According to the pairing model, one would expect to find among the transition states no two-quasiparticle excitation until the available energy exceeds  $2\Delta_0 \approx 2.30$  MeV. Indeed, aside from some few collective vibrational excitations and their rotational bands, one expects to find only the rotational states of the ground-state band (with  $K = 0$ ) up to this minimum two-quasiparticle energy. Above  $2\Delta_0$ , on the other hand, the two-quasiparticle states should immediately become numerically dominant.<sup>4</sup> This sudden change of character would reflect itself in a sudden increase from  $K_0^2 \approx 0$  to  $K_0^2 \approx 2\langle k_p^2 \rangle_{av} \approx 16$  to 22, where  $\langle k_p^2 \rangle_{av}$  is the mean square value  $K$  for the last filled single-particle states. The steep rise in  $K_0^2$  for  $\text{Pu}^{240}$  at  $E^* - E_f \approx 2.6$  MeV is quite consistent with this picture and should, we believe, be interpreted as direct evidence that  $2\Delta_0 = 2.6_{-0.45}^{+0.21}$  MeV,<sup>21</sup> a value consistent with that mentioned above. This can be compared with the average gap,<sup>20</sup> 1.2 MeV, or with the larger (neutron) gap, 1.5 MeV, in the spectrum of  $\text{Pu}^{240}$  near its stable-state shape.

One might inquire why the energy gap should be larger at the highly deformed saddle-point shape than at the ground-state shape. One possible answer is that the pairing effect in nuclei is essentially a finite-size effect, depending for a given nucleus upon the surface-to-volume ratio of the shape in question. Such an explanation is indicated by the work of Kennedy *et al.*<sup>22</sup> who studied pairing effects as a function of thickness in an infinite (in two dimensions) slab of nuclear matter.

<sup>18</sup> J. E. Simmons, R. L. Henkel, and R. B. Perkins, Phys. Rev. **137**, B809 (1965).

<sup>19</sup> J. Simmons and R. Henkel, Phys. Rev. **120**, 198 (1960).

<sup>20</sup> S. G. Nilsson and O. Prior, Kgl. Danske Videnskab. Selskab. Mat. Fys. Medd. **32**, No. 16 (1960). Figures 9 and 10 imply that  $\Delta_0 = 0.6$  MeV is an appropriate average of the neutron and proton gaps in  $\text{Pu}^{240}$ .

<sup>21</sup> The quoted uncertainties represent the uncertainty ( $\pm 0.25$  MeV) in estimating the position of the two-quasiparticle threshold energy and the possible error in the definition of the threshold energy ( $< 0.2$  MeV; Cf. Ref. 10.). In a preliminary report of this work, Phys. Rev. Letters **11**, 343 (1963), a value  $2\Delta_0 \approx 2.7$  MeV was given. The difference of 0.1 MeV from the present value came from a reanalysis of the data.

<sup>22</sup> R. C. Kennedy, L. Wilets, and E. M. Henley, Phys. Rev. Letters **12**, 36 (1964).

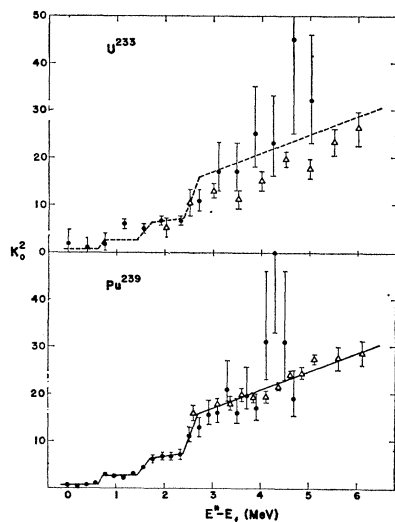


FIG. 7. Values of  $K_0^2$  (solid points) calculated from measured values of  $g_2$  by means of the theory developed in the text. The triangles are from neutron data and its analysis for  $\text{Pu}^{239}$  can be found in Griffin (Ref. 6) and Simmons *et al.* (Ref. 18); for  $\text{U}^{233}$ , see Simmons and Henkel (Ref. 19).

It would also be consistent with the results of studies of pairing effects in infinite nuclear matter,<sup>23,24</sup> which give a nuclear pairing effect much smaller than that observed in stable nuclei.

There also occurs in Fig. 7 evidence for two smaller increases in  $K_0^2$  at energies 0.7 and 1.6 above the fission threshold. The suggestion has been advanced<sup>25</sup> that this behavior is qualitatively consistent with excited vibrational states analogous to the  $\gamma$  vibrations of deformed nuclei about their stable shapes. The simplest  $\gamma$  vibration has  $K = \pm 2$ . The value  $K_0^2 \approx 3$  inferred for  $0.7 < E^* - E_f < 1.6$  MeV therefore corresponds well with a situation where fission is occurring through transition states of this kind, as well as through higher rotational states of the ground-state ( $K=0$ ) band. Similarly, a double  $\gamma$ -vibrational excitation would be expected to occur at about twice that excitation energy. There would then occur a triplet of excited states with  $K = \pm 4, 0$ . The value  $K_0^2 \approx 7$  observed for  $1.6 < E^* - E_f < 2.6$  MeV is consistent with fission through such barrier states as well as through higher rotational members of the  $K=0$  and  $K=2$  bands discussed above. Although only a speculation, this suggestion is interesting in pointing out the role of the larger pairing gap for the observation, and perhaps even for the existence, of "multiphonon" vibrational states: in nuclei with equilibrium deformation, such states occur at energies where two quasiparticle states would normally be avail-

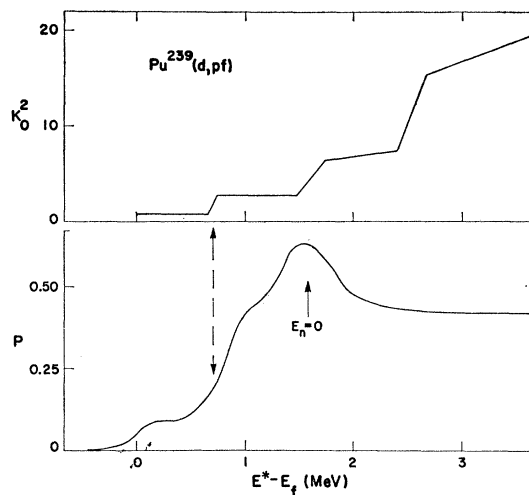


FIG. 8. Comparison between the variation of  $K_0^2$  and the fission-barrier penetrability  $P$ .

able to mix with the collective state or at least to obscure it for the experimentalist.

A comparison can be made between the behavior of  $K_0^2$  from the present experiment and the previously measured variation of fission-barrier penetrability.<sup>1</sup> In Fig. 8 the lines which have been drawn through the data points of the two experiments are plotted on the same scale of excitation. This figure emphasizes that *both* types of data show an increase at about 0.7-MeV excitation above the fission barrier, corresponding to the suggested onset of a vibrational band. A similar correlation at  $E^* - E_f = 1.6$  and 2.6 MeV is obscured in the penetrability data by the beginning of both neutron emission and deuteron breakup.

The conclusions of the present paper may contribute to the interpretation of *neutron* fission cross sections. Specifically, it is interesting to look for possible effects of the pairing energy gap in the well-determined data<sup>26</sup> for  $\text{Pu}^{239}$ . Indeed, these data show an inflection in cross section from a plateau value of 1.65 b below 1 MeV, to 2.0 b above. This change is rather well centered at 1 MeV, an energy which produces 2.6-MeV excitation energy in the fissioning  $\text{Pu}^{240}$  nucleus. The corresponding large increase of  $K_0^2$  at this energy suggests that this increase in cross section results from the onset of quasiparticle excitations.

As noted in Sec. 3, the data for  $\text{U}^{234}$  fission are inferior statistically to those for  $\text{Pu}^{240}$ . In Fig. 7 the same curve (dotted) has been drawn through the  $\text{U}^{234}$  data as was given by the  $\text{Pu}^{240}$  case to indicate that there is no evidence for a qualitative difference between the  $K_0^2$  behavior for these two nuclides, and that the difference in the observed anisotropies is adequately accounted for by the difference in target spins.

<sup>23</sup> V. J. Emery and A. M. Sessler, Phys. Rev. **119**, 248 (1960).

<sup>24</sup> E. M. Henley and L. Wilets, Phys. Rev. Letters **11**, 326 (1963).

<sup>25</sup> J. J. Griffin and M. Rich, Bull. Am. Phys. Soc. **8**, 525 (1963).

<sup>26</sup> R. L. Henkel, Los Alamos Scientific Laboratory Report No. LA-2114, 1957 (unpublished).